Original Article

Comprehensive analysis reveals *CTHRC1*, *SERPINE1*, *VCAN* and *UPK1B* as the novel prognostic markers in gastric cancer

Zhipeng Zhu[1#], Jiuhua Xu[2#], Lulu Li[1#], Weipeng Ye[2], Borong Chen[1], Junjie Zeng[1], Zhengjie Huang[1,2]

[1]Department of Gastrointestinal Surgery, Xiamen Cancer Center, The First Affiliated Hospital of Xiamen University, Xiamen, China; [2]Department of clinical medicine, Fujian Medical University, Fuzhou, China

Contributions: (I) Conception and design: Z Zhu; (II) Administrative support: Z Huang; (III) Provision of study materials or patients: Z Zhu; (IV) Collection and assembly of data: L Li, J Xu; (V) Data analysis and interpretation: W Ye, B Chen, J Zeng; (VI) Manuscript writing: All authors; (VII) Final approval of manuscript: All authors.

[#]These authors contributed equally to this work.

Correspondence to: Dr. Zhengjie Huang. Department of Gastrointestinal Surgery, Xiamen Cancer Center of The First Affiliated Hospital of Xiamen University, 55 Zhen Hai Road, Si Ming District, Xiamen, China. Email: huangzhengjie@xmu.edu.cn.

Background: Gastric cancer (GC) is one of the most common malignant diseases worldwide, the incidence and mortality for GC is still high, thus it is urgently important to identify the effective and reliable biomarkers to evaluate GC and the underlying molecular events.

Methods: The study integrated four Gene Expression Omnibus (GEO) profile datasets and The Cancer Genome Atlas (TCGA) dataset to screen differentially expressed genes (DEGs), screened key genes by performing the Kaplan-Meier analysis, univariate and multivariate-cox analysis. Further analysis were performed to evaluate and validate the prognostic value of the key genes based on TCGA database and online websites. In addition, mechanism analysis of the key genes was performed thought biological processes and KEGG pathway analysis.

Results: In the study, 192 DEGs (92 up-regulated and 100 down-regulated) were identified from the GEO and TCGA datasets. Next, gene ontology (GO) for DEGs focused primarily on cell adhesion, extracellular region and extracellular matrix structural constituent. Then four significant key genes were screened by performed the Kaplan-Meier analysis, univariate and multivariate-cox analysis. By using Kaplan-Meier plotter and OncoLnc, the expression level was associated with a worse prognosis. In addition, the area under curve (AUC) for time-dependent receiver operating characteristic (ROC) indicated a moderate diagnostic value. Furthermore, the expression of collagen triple helix repeat containing 1 (*CTHRC1*), serpin family E member 1 (*SERPINE1*), *Versican* (*VCAN*) was associated with tumor size, *Uroplakin 1B* (*UPK1B*) expression was associated with distant metastasis. Finally, multiple biological processes and signaling pathway associated with key genes revealed the underlying mechanism in GC.

Conclusions: Taken together, *CTHRC1*, *SERPINE1*, *VCAN*, *UPK1B* were novel potential prognostic molecular markers for GC, which acted as oncogene to promote the development of GC.

Keywords: Gastric cancer (GC); data mining; prognostic markers

Submitted Jan 06, 2020. Accepted for publication Jun 05, 2020.
doi: 10.21037/tcr-20-211
View this article at: http://dx.doi.org/10.21037/tcr-20-211

Introduction

The incidence and mortality for gastric cancer (GC) have been appreciably declining for several decades. However, GC is still the fourth most common cancer and the second leading cause of cancer deaths worldwide (1-3). In China alone, there were about 679/100,000 of new GC cases and 798/100,000 of death GC cases and accounting for

Table 1 Details for GEO gastric cancer data

Reference	Sample	GEO	Platform	Normal	Tumor
He *et al.*	Gastric cancer	GSE79973	GPL570	10	10
Oh *et al.*	Gastric cancer	GSE63089	GPL5175	45	45
Hippo *et al.*	Gastric cancer	GSE54129	GPL570	21	111
Siegel *et al.*	Gastric cancer	GSE26899	GPL6947	12	96

GEO, Gene Expression Omnibus.

the third of malignant tumor incidence and mortality in 2015 (4). The pathogenesis of GC is multifactorial, including genetic susceptibility and environmental factors, cell cycle, DNA repair, metabolism, cell-to-cell and cell-to-matrix interactions, apoptosis, angiogenesis, and immune surveillance contribute to cancer development (5). However, although there have been extensive previous studies on the molecular mechanism of GC formation and progression, the molecular mechanism of GC is not yet clear. Due to high morbidity and mortality in GC, it is urgently important to reveal the causes and the underlying molecular mechanisms. Thus, identifying novel diagnostic and prognostic biomarkers remains critical importance for stomach cancer.

In this work, we have downloaded four original microarray datasets GSE79973 (6), GSE26899 (7), GSE54129 (8), GSE63089 (9), from NCBI-Gene Expression Omnibus database (NCBI-GEO), there are total of 262 GC cases and 88 normal cases available. differentially expressed genes (DEGs) between cancer tissues and normal tissues were obtained from GEO and TCGA gene expression profile, respectively. Then, we overlapped the four GEO and TCGA gene expression profiles and identified 204 overlapped genes, DAVID was used to perform GO enrichment analysis and KEGG enrichment analysis on the overlapped genes. Next, some analysis has been performed to screen the key genes, including: the Kaplan-Meier analysis, univariate and multivariate-cox analysis for overall survival (OS). In addition, to evaluate and validate the prognostic value of the key genes, we performed the correlation analysis between TMN and expression of key genes based on TCGA data, the Kaplan-Meier analysis based on the online website including Kaplan-Meier plotter and OncoLnc, ROC analysis for OS and DFS, univariate and multivariate-cox analysis for DFS. Furthermore, the co-expressed genes associated with GC were identified by using Coexpedia, the biological processes and KEGG-signaling pathway were predicted via using R software. Finally, Gene set enrichment analysis (GSEA) was performed to further investigate pathways of four key genes that may be associated with GC.

Methods

Identification and processing of microarray data

We used the "GC" OR "gastric carcinoma" keyword to search gene expression profiles from GEO database (http://www.ncbi.nlm.nih.gov/geo/), and four qualified gene expression profiles (GSE54129, GSE79973, GSE63089, GSE26899) were identified with platform and series matrix file(s) being downloaded as TXT files, type of data were RMA signal intensity and standardized, and log2 transformed. The dataset information was presented in *Table 1*.

Identification of DEGs and overlapped genes

R annotation package was performed to convert the probe into gene symbol. Next, SVA package was used for background correction, merge package was applied to combine the four gene expression data according to the gene symbol. Then, gene differential expression analysis between normal cases and tumor cases was performed by using limma package in the Bioconductor package from GEO and TCGA gene expression profile, with corrected P value <0.05 and absolute log fold change (FC) >1 being considered as the cutoff criterion. Finally, overlapped genes were identified from four GEO and TCGA gene expression profiles.

Overlapped genes enrichment analysis

The DAVID database (https://david.ncifcrf.gov/) is an essential foundation for the success of any high-throughput gene function analysis. We used DAVID to perform GO annotations analysis on overlapped genes.

Identification and validation of clinically relevant hub genes

The Kaplan-Meier analysis was performed to screen the survival-related genes, univariate and multivariate-cox analysis for OS was conducted to identify the key genes from the survival-related genes. To evaluate and validate the prognostic value of the key genes, we performed the Kaplan-Meier analysis based on the online website including Kaplan-Meier plotter (http://kmplot.com/) and OncoLnc (http://www.oncolnc.org/). The Kaplan-Meier analysis for disease free survival (DFS) based on TCGA dataset, univariate and multivariate-cox analysis for DFS by mining TCGA dataset, the receiver operating characteristic (ROC) analysis for OS and DFS, the correlation analysis between TMN and expression of key genes based on TCGA data. The gene expression level ≤ median was regarded as low expression, otherwise was regarded as high expression.

Biological processes and signaling pathway analysis for the co-expressed genes associated with GC

To explore the potential mechanisms for the key genes, we identified the co-expressed genes associated with key genes by using Coexpedia (http://www.coexpedia.org/), biological processes and KEGG-signaling pathway for the co-expressed genes associated with GC were predicted by R software.

Gene set enrichment analysis

To further investigate pathways of four key genes that may be associated with GC, GSEA was performed using the JAVA program (http://www.broadinstitute.org/gsea) with TCGA dataset. Expression of each key gene was set to annotate phenotypes, 1,000 times were performed for gene set permutations. The nominal P value <0.05 was used to sort the pathways enriched in each phenotype.

Results

The DEG of GEO gene expression profiles

We performed background correction on the GEO expression profiles. The result was shown in *Figure 1*. Then, we analyzed the DEGs of integrated GEO and TCGA gene expression profiles by using the limma package (FDR <0.05, absolute log FC >1), 219 up-regulated genes and 179 down-regulated genes were obtained from GSE26899, GSE54129, GSE63089 and GSE79973, 1,110 up-regulated genes and 1566 down-regulated genes were obtained from TCGA dataset. After using Venny, 92 up-regulated genes and 100 down-regulated genes were overlapped across four GEO and TCGA datasets (*Figure 2*).

GO and KEGG enrichment analysis

Enrichment analysis of the overlapped genes was performed using the DAVID online site (corrected P value<0.05). The enrichment analysis was divided into three functional groups, including biological processes, cell composition and molecular function, biological processes. In the biological processes group, the differential genes were mainly enriched in cell adhesion and biological adhesion. In the cell composition, the differential genes were mainly enriched in the extracellular region and the extracellular region part. In the molecular function, the differential genes were mainly enriched in the extracellular matrix structural constituent and pattern binding (*Figure 3*).

Identification of four key genes from overlapped genes

Twenty-three survival-related genes were identified by performing the Kaplan-Meier analysis, and high expression level was associated with a poorer OS (*Table S1*).Then, we identified four significant key genes by conducting univariate and multivariate-Cox analysis for OS, including *CTHRC1*, *SERPINE1*, *UPK1B* , *VCAN*, with HR >1 (P<0.05) (*Figure 4*).

Prognostic significance for the four genes

The gene expression of the cancer group was higher than the normal group from TCGA dataset for *CTHRC1* (*Figure 5A*), *SERPINE1* (*Figure 5B*), *UPK1B* (*Figure 5C*) and *VCAN* (*Figure 5D*). Meantime, the gene expression of the cancer group was higher than paracancerous group for *CTHRC1* (*Figure 5E*), *SERPINE1* (*Figure 5F*), *UPK1B* (*Figure 5G*) and *VCAN* (*Figure 5H*). By using OncoLnc, it indicated high gene expression was significantly associated with a shorter OS (*Figure 6A,B,C,D*). Then Kaplan Meier plotter revealed the same trend, high expression presented worse OS (*Figure 6E,F,G,H*), first progression (FP) (*Figure 6I,J,K,L*) and post progression survival (PPS) (*Figure 6M,N,O,P*). Next, the ROC analysis of four key genes was performed to evaluate the diagnostic value of four key genes for OS, as showed in *Figure 7*, all the AUC indicated a moderate diagnostic

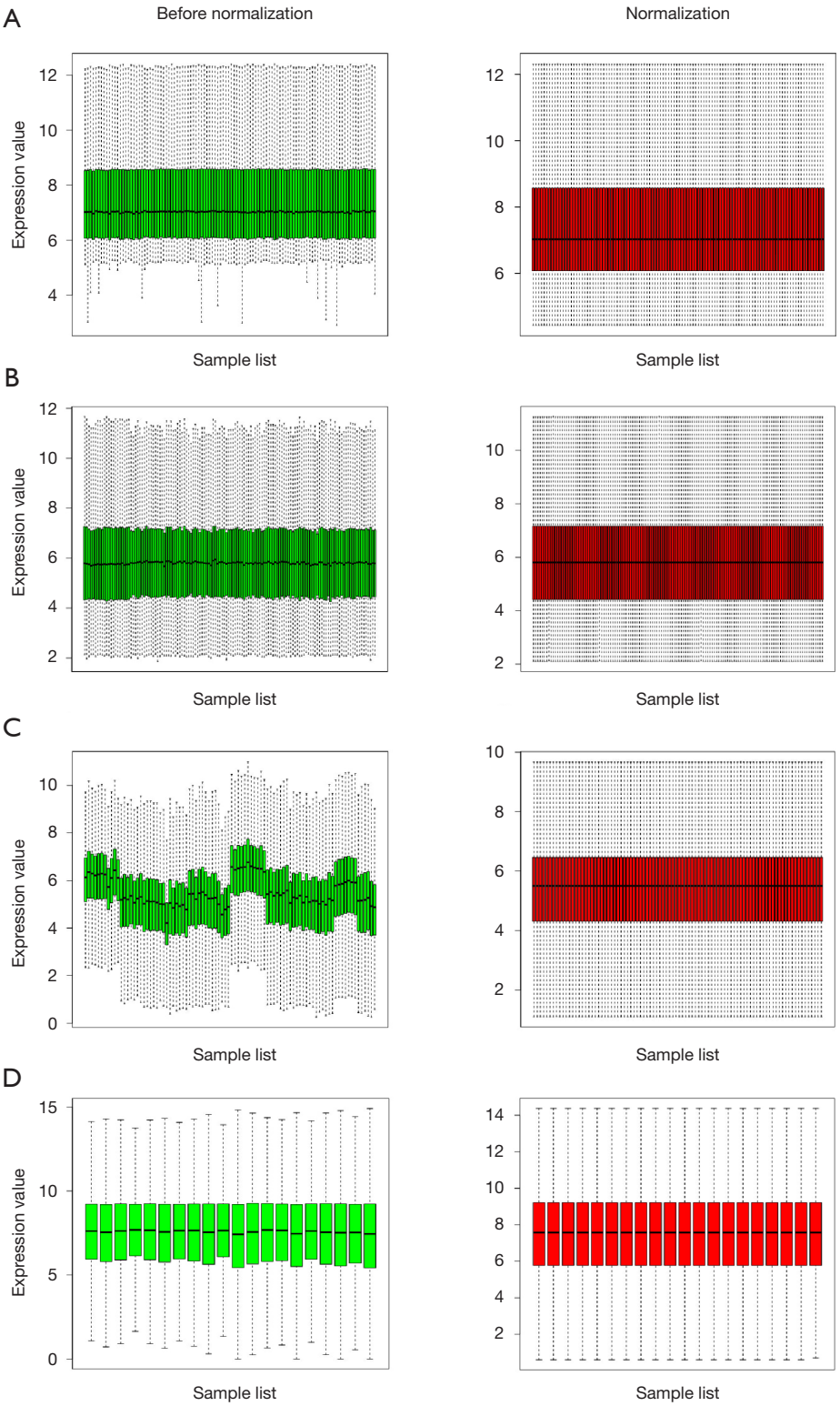

Figure 1 Standardization of gene expression. (A) The standardization of GSE26899 data, (B) the standardization of GSE54129 data, and (C) the standardization of GSE63089 data. (D) the standardization of GSE79973 data. The green bar represents the data before normalization, and the red bar represents the normalized data.

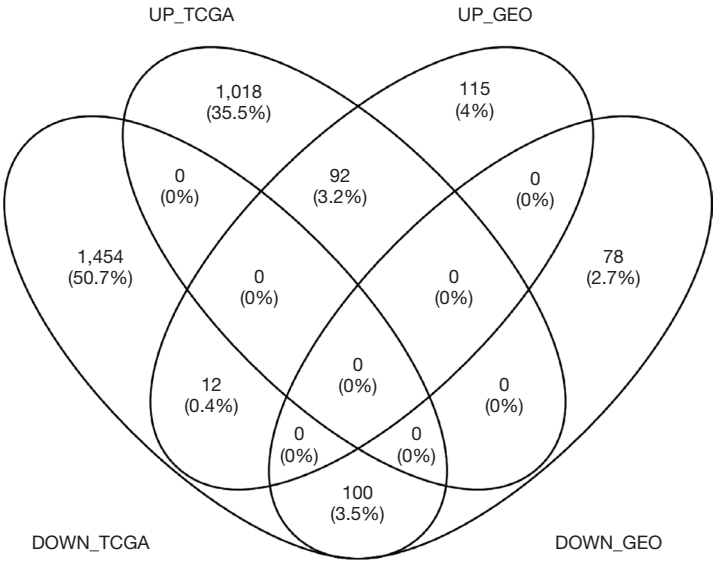

Figure 2 Venn plot of the DEGs between the integrated four GEO datasets and the TCGA dataset. DEGs, differentially expressed genes; GEO, Gene Expression Omnibus; TCGA, The Cancer Genome Atlas.

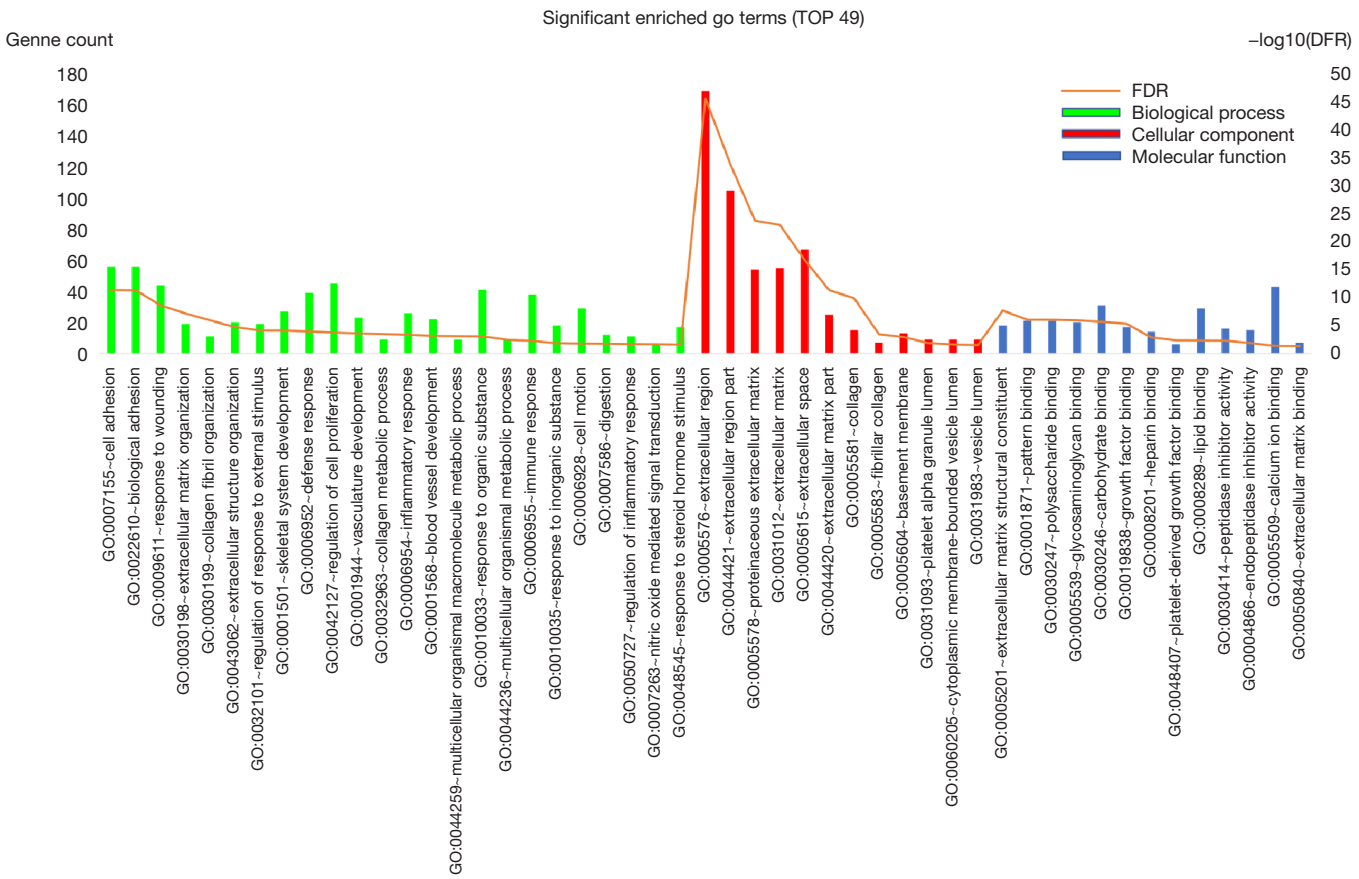

Figure 3 GO enrichment analysis of overlapped genes into three functional groups: molecular function, biological processes, and cell composition. GO, gene ontology.

A

Factors	Univariate Cox-regression analysis			Multivariate Cox-regression analysis		
	HR	95%CI	P-value	HR	95%CI	P-value
Age	1.028	1.0091–1.0473	0.0036	1.0347	1.0148–1.055	0.0006
Gender	1.4923	0.9935–2.2415	0.0538			
Grade	1.4189	0.9873–2.0394	0.0587			
Tumor size (cm)	1.2535	0.9969–1.576	0.0531			
Metastasis	2.0319	1.0891–3.7906	0.0259	2.6655	1.3957–5.0906	0.003
Lymph node	1.2851	1.0880–1.5178	0.0031	1.306	1.1026–1.547	0.002
CTHRC1 (high/low)	1.6083	1.1130–2.324	0.0113	1.6199	1.1143–2.3548	0.0115

B

Factors	Univariate Cox-regression analysis			Multivariate Cox-regression analysis		
	HR	95%CI	P-value	HR	95%CI	P-value
Age	1.028	1.0091–1.0473	0.0036	1.0345	1.0144–1.0549	0.0007
Gender	1.4923	0.9935–2.2415	0.0538			
Grade	1.4189	0.9873–2.0394	0.0587			
Tumor size (cm)	1.2535	0.9969–1.576	0.0531			
Metastasis	2.0319	1.0891–3.7906	0.0259	2.6205	1.3733–50004	0.0035
Lymph node	1.2851	1.0880–1.5178	0.0031	1.3356	1.128–1.5814	0.0008
SERPINE1 (high/low)	1.7616	1.2142–2.5557	0.0029	1.5497	1.0682–2.2483	0.021

C

Factors	Univariate Cox-regression analysis			Multivariate Cox-regression analysis		
	HR	95%CI	P-value	HR	95%CI	P-value
Age	1.028	1.0091–1.0473	0.0036	1.0381	1.0181–1.0585	0.0002
Gender	1.4923	0.9935–2.2415	0.0538			
Grade	1.4189	0.9873–2.0394	0.0587			
Tumor size (cm)	1.2535	0.9969–1.576	0.0531			
Metastasis	2.0319	1.0891–3.7906	0.0259	2.4464	1.2849–4.6577	0.0065
Lymph node	1.2851	1.0880–1.5178	0.0031	1.3091	1.1048–1.5511	0.0019
UPK1B (high/low)	1.8657	1.286–2.7068	0.001	1.8243	1.2555–2.6509	0.0016

D

Factors	Univariate Cox-regression analysis			Multivariate Cox-regression analysis		
	HR	95%CI	P-value	HR	95%CI	P-value
Age	1.028	1.0091–1.0473	0.0036	1.0378	1.0176–1.0585	0.0002
Gender	1.4923	0.9935–2.2415	0.0538			
Grade	1.4189	0.9873–2.0394	0.0587			
Tumor size (cm)	1.2535	0.9969–1.576	0.0531			
Metastasis	2.0319	1.0891–3.7906	0.0259	2.9	1.5128–5.5593	0.0013
Lymph node	1.2851	1.0880–1.5178	0.0031	1.3103	1.106–1.5523	0.0018
VCAN (high/low)	1.7418	1.2017–2.5246	0.0034	1.8005	1.2372–2.6205	0.0021

Figure 4 Univariate and multivariate analysis of clinicopathologic characteristics and key genes for OS. (A) *CTHRC1* (B) *SERPINE1* (C) *UPK1B* (D) *VCAN*. OS, overall survival; *CTHRC1*, collagen triple helix repeat containing 1; *SERPINE1*, plasminogen activator inhibitor type 1; *UPK1B*, uroplakin Ib; *VCAN*, Verscan.

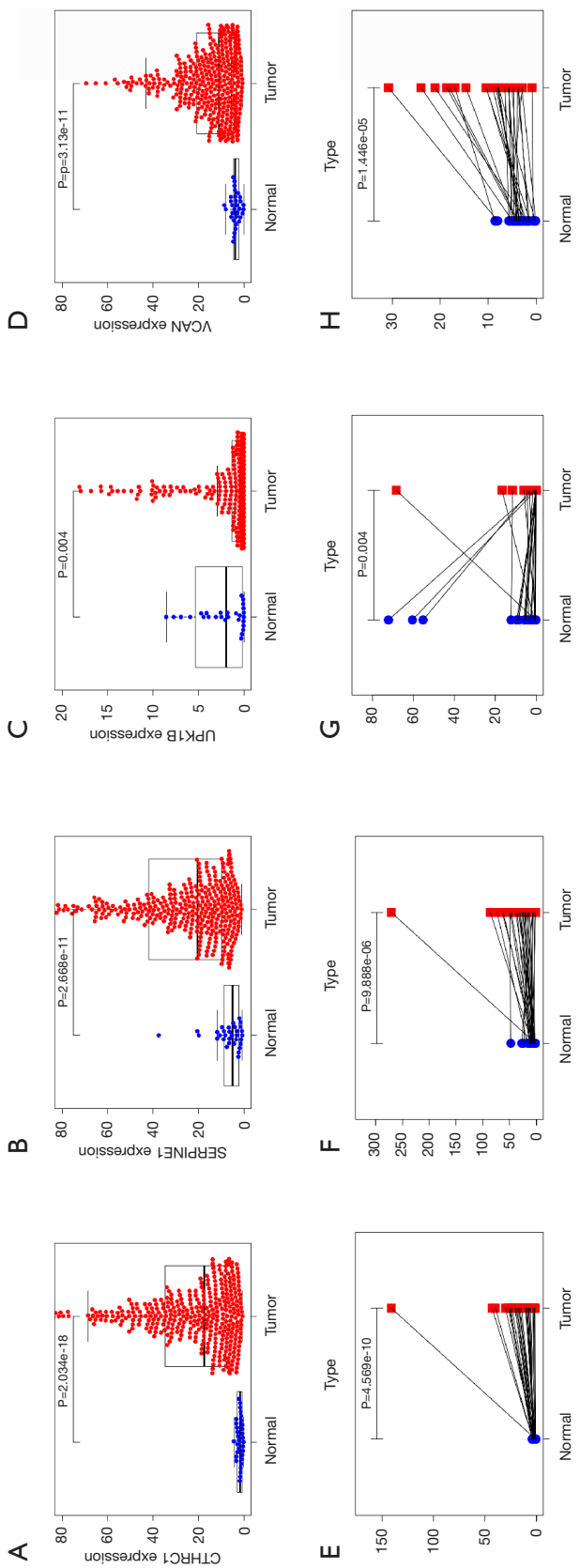

Figure 5 Comparation of the key gene expression. The different expression level in normal tissue and GC (A-D), (A) *CTHRC1*, (B) *SERPINE1*, (C) *UPK1B*, (D) *VCAN*. The different expression level in paracancerous tissue and GC (E-H), (E) *CTHRC1*, (F) *SERPINE1*, (G) *UPK1B*, (H) *VCAN*. *CTHRC1*, collagen triple helix repeat containing 1; *SERPINE1*, plasminogen activator inhibitor type 1; *UPK1B*, uroplakin Ib; *VCAN*, Verscan.

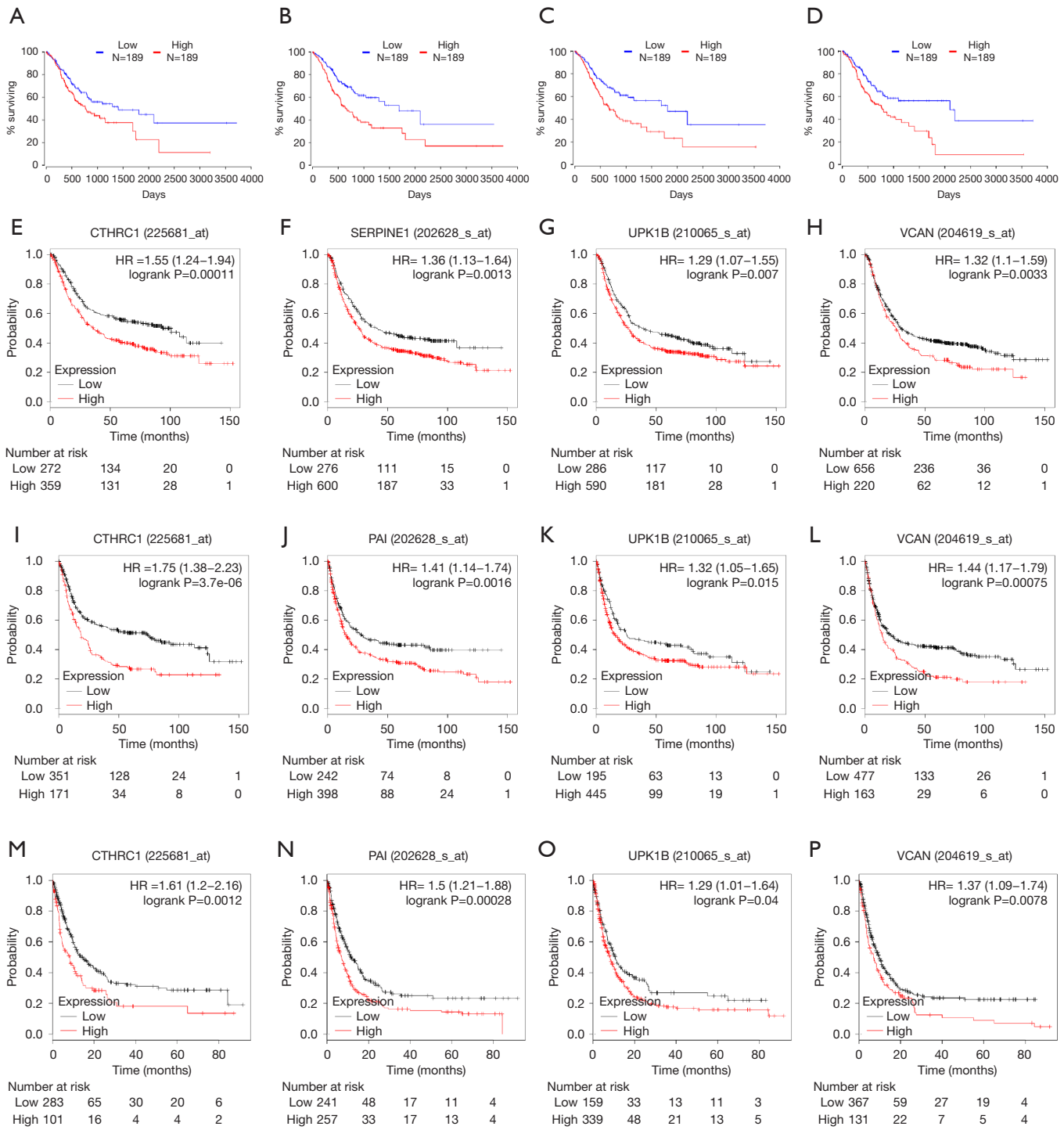

Figure 6 The performance analysis using OncoLnc (A-D) and Kaplan-Meier Plotter (E-P), (E-H) OS, (I-L) FP, (M-P) PPS. (A,E,I,M) *CTHRC1*, (B,FJ,N) *SERPINE1*, (C,G,K,O) *UPK1B*, (D,H,L,P) *VCAN*. *CTHRC1*, collagen triple helix repeat containing 1; *SERPINE1*, plasminogen activator inhibitor type 1; *UPK1B*, uroplakin Ib; *VCAN*, Verscan; GC, gastric cancer.

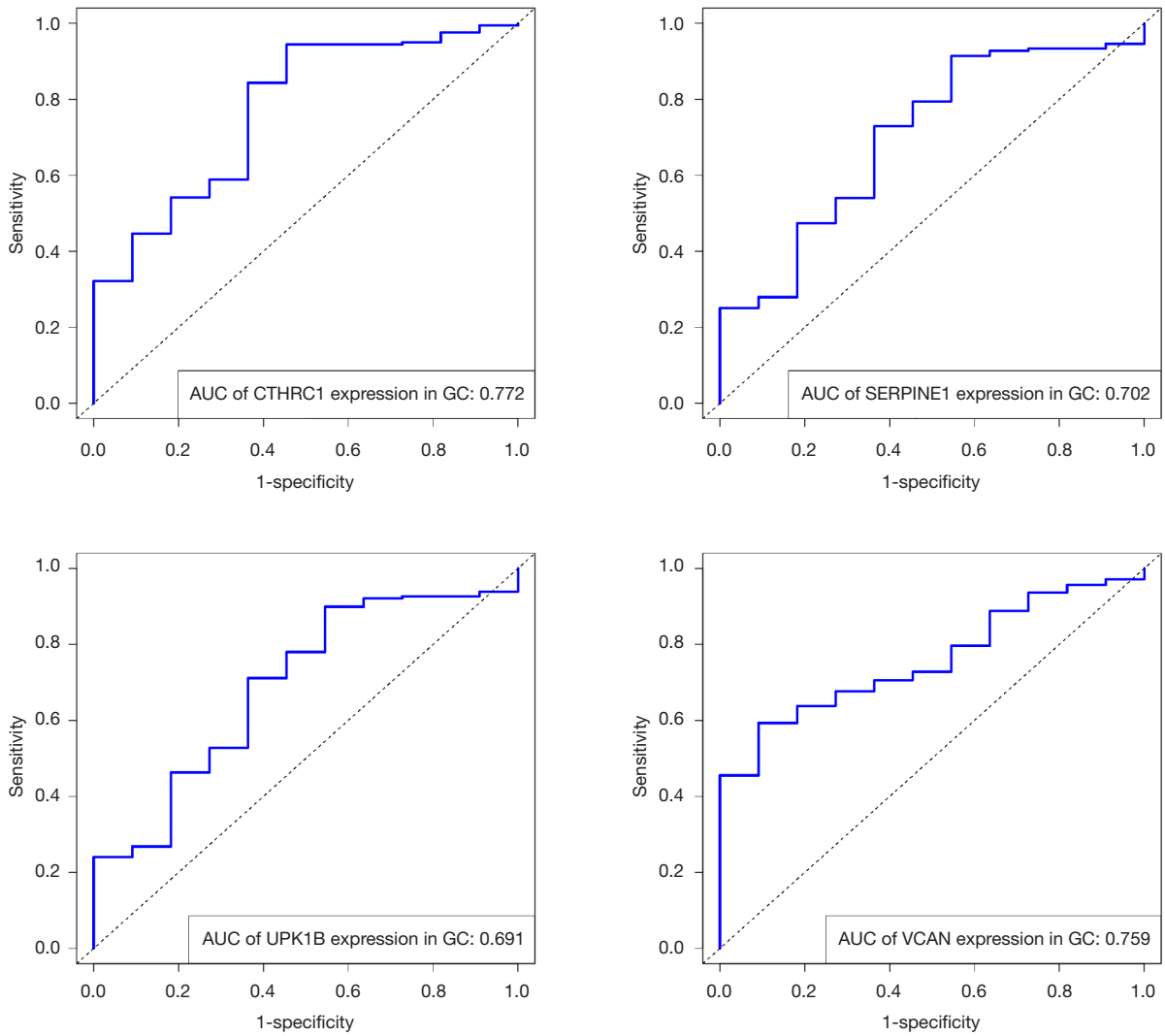

Figure 7 The ROC curve for OS in GC. ROC, Time-dependent receiver operating characteristic; OS, overall survival; GC, gastric cancer.

value (*CTHRC1*: 0.772, *SERPINE1*: 0.702, *UPK1B*: 0.691, *VCAN*: 0.759). Furthermore, patients with high expression level have poorer DFS than the patients with low expression level (P<0.05, *Figure 8A,B,C,D*). The ROC curve for DFS demonstrated that CTHRC1, SERPINE1, UPK1B and VCAN were specific and sensitive than any clinical characteristics, including age, gender, grade, tumor size, lymph node and metastasis (*Figure 8E,F,G,H*). In addition, univariate and multivariate-Cox analysis for DFS displayed four key genes were all powerful and independent factors for DFS (*Figure 9*). Finally, correlation analysis between TMN and expression of key genes was analyzed by performing Mann-Whitney-Wilcoxon Test based on TCGA data, it revealed that gene expression was associated with tumor stage, including *CTHRC1*, *SERPINE1*, *VCAN*. Meantime, *UPK1B* expression was associated with distant metastasis (*Figure 10*).

Biological processes and signaling pathway analysis for the co-expressed genes associated with GC

We identified the co-expressed genes associated with key genes in GC. In addition, the biological processes and signaling pathway analysis of key genes in GC were investigated. These co-expressed genes were involved in a variety of biological processes, such as endodermal cell

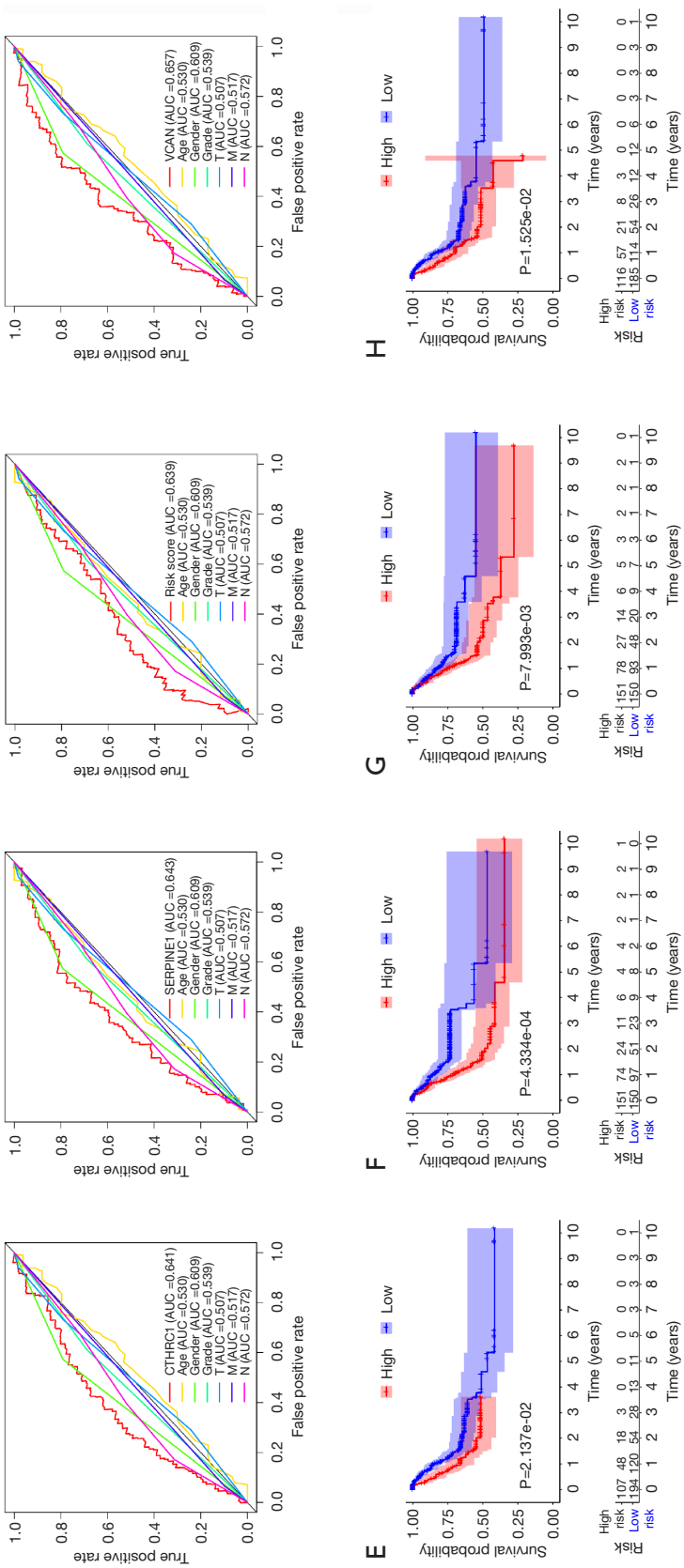

Figure 8 The performance analysis for DFS in GC. The ROC curve for DFS in GC (A-D), Kaplan-Meier plotter for DFS in GC (E-H). (A,E) *CTHRC1*, (B,F) *SERPINE1*, (C,G) *UPK1B*, (D,H) *VCAN*. *CTHRC1*, collagen triple helix repeat containing 1; *SERPINE1*, plasminogen activator inhibitor type 1; *UPK1B*, uroplakin Ib; *VCAN*, Verscan; GC, gastric cancer.

A

Factors	Univariate Cox-regression analysis			Multivariate Cox-regression analysis		
	HR	95%CI	P-value	HR	95%CI	P-value
Age	0.9876	0.9687–1.0068	0.2049			
Gender	2.154	1.3217–3.5103	0.0021	2.0844	1.2767–3.4032	0.0033
Grade	1.3957	0.9248–2.1066	0.1124			
Tumor size (cm)	1.1034	0.8613–1.4136	0.4362			
Metastasis	1.4179	0.6182–3.2525	0.4097			
Lymph node	1.3449	1.1145–1.6228	0.002	1.3471	1.117–1.6246	0.0018
CTHRC1 (high/low)	1.4842	1.2726–2.2648	0.0047	1.4172	1.0271–2.1 664	0.0411

B

Factors	Univariate Cox-regression analysis			Multivariate Cox-regression analysis		
	HR	95%CI	P-value	HR	95%CI	P-value
Age	0.9876	0.9687–1.0068	0.2049			
Gender	2.154	1.3217–3.5103	0.0021	2.0091	1.23–3.2817	0.0053
Grade	1.3957	0.9248–2.1066	0.1124			
Tumor size (cm)	1.1034	0.8613–1.4136	0.4362			
Metastasis	1.4179	0.6182–3.2525	0.4097			
Lymph node	1.3449	1.1145–1.6228	0.002	1.3475	1.1172–1.6253	0.0018
SERPINE1 (high/low)	2.1124	1.3793–3.235	0.0006	1.9966	1.302–3.0619	0.0015

C

Factors	Univariate Cox-regression analysis			Multivariate Cox-regression analysis		
	HR	95%CI	P-value	HR	95%CI	P-value
Age	0.9876	0.9687–1.0068.	0.2049			
Gender	2.154	1.3217–3.5103	0.0021	2.1743	1.3335–3.5451	0.0018
Grade	1.3957	0.9248–2.1066	0.1124			
Tumor size (cm)	1.1034	0.8613–1.4136	0.4362			
Metastasis	1.4179	0.6182–3.2525	0.4097			
Lymph node	1.3449	1.1145–1.6228	0.002	1.3151	1.0886–1.5888	0.0045
UPK1B (high/low)	1.7957	1.1783–2.7366	0.0065	1.6956	1.1104–2.5892	0.0145

D

Factors	Univariate Cox-regression analysis			Multivariate Cox-regression analysis		
	HR	95%CI	P-value	HR	95%CI	P-value
Age	0.9876	0.9687–1.0068	0.2049			
Gender	2.154	1.3217–3.5103	0.0021	2.0358	1.245–3.329	0.0046
Grade	1.3957	0.9248–2.1066	0.1124			
Tumor size (cm)	1.1034	0.8613–1.4136	0.4362			
Metastasis	1.4179	0.6182–3.2525	0.4097			
Lymph node	1.3449	1.1145–1.6228	0.002	1.3374	1.1101–1.6112	0.0022
VCAN (high/low)	1.6653	1.0981–2.5256	0.0164	1.5353	1.0088–2.3364	0.0454

Figure 9 Univariate and multivariate analysis of clinicopathologic characteristics and key genes for DFS. (A) *CTHRC1*, (B) *SERPINE1*, (C) *UPK1B*, (D) *VCAN*. DFS, disease free survival; *CTHRC1*, collagen triple helix repeat containing 1; *SERPINE1*, plasminogen activator inhibitor type 1; *UPK1B*, uroplakin Ib; *VCAN*, Verscan.

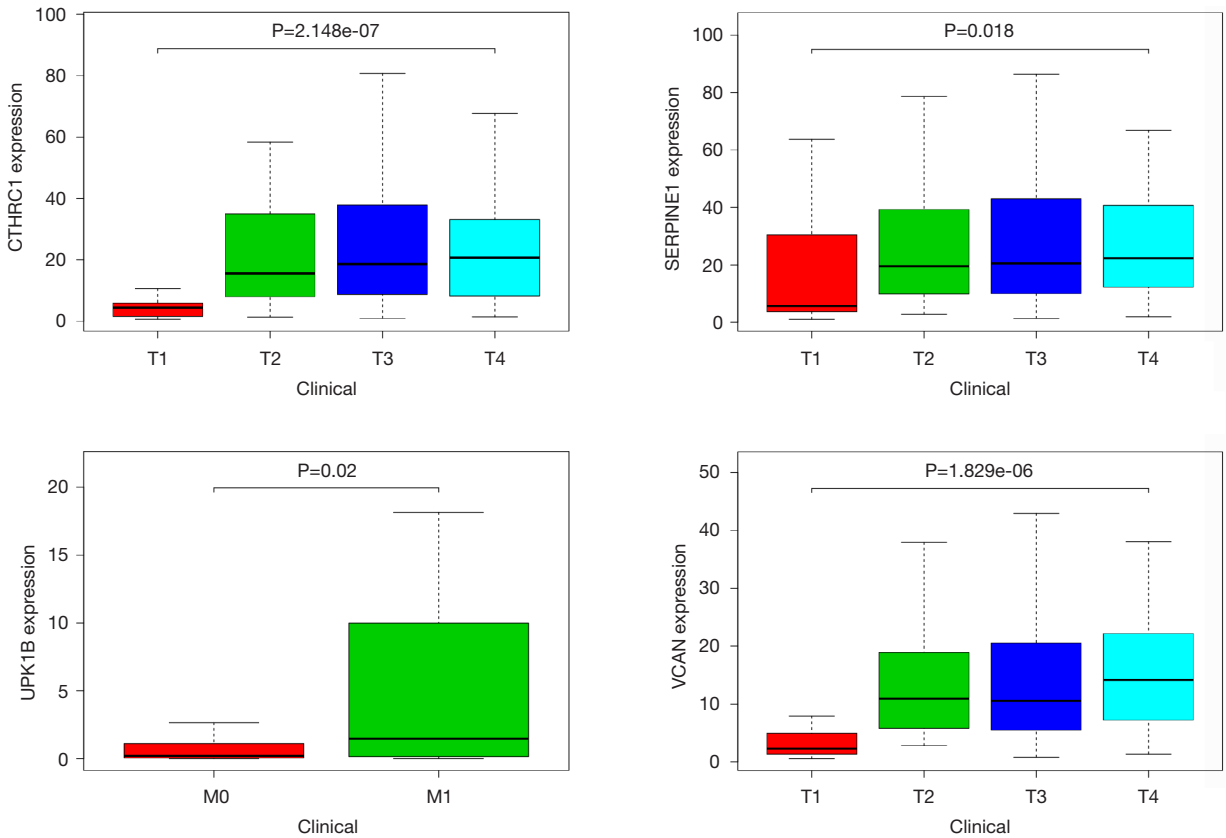

Figure 10 Significant correlation between key gene expression and TMN in GC. T, tumor; N, lymph node; M, metastasis; GC, gastric cancer.

differentiation, endoderm development, and extracellular matrix organization for *CTHRC1* (*Figure 11A*), regulation of angiogenesis, positive regulation of leukocyte chemotaxis cellular, and regulation of vasculature development for *SERPINE1* (*Figure 11B*), extracellular matrix organization, collagen fibril organization, collagen metabolic process, and endodermal cell differentiation for *UPK1B*, extracellular matrix organization, and cellular response to transforming growth factor beta stimulus for *VCAN*. These co-expressed genes were involved in a variety of biological processes, such as ECM-receptor interaction, AGE-RAGE signaling pathway in diabetic complications, PI3K-Akt signaling pathway for *CTHRC1* (*Figure 12A*), such as NF-kappa B signaling pathway, PI3K-Akt signaling pathway, Toll-like receptor signaling pathway for *SERPINE1* (*Figure 12B*), such as ECM-receptor interaction, PI3K-Akt signaling pathway, relaxin signaling pathway for *UPK1B* (*Figure 12C*), such as ECM-receptor interaction, PI3K-Akt signaling pathway for *VCAN* (*Figure 12D*).

GSEA identifies prognostic genes-related signaling pathway

In order to further explore the mechanism of prognostic genes in patients with GC, we conducted GSEA between low and high expression group to identify the significant pathways (FDR <0.05, NOM P value <0.05). For *CTHRC1*, some significant pathways which were active in the high-expression group, including KEGG_ECM_RECEPTOR_INTERACTION, KEGG_CYTOKINE_CYTOKINE_RECEPTOR_INTERACTION, KEGG_TGF_BETA_SIGNALING_PATHWAY, KEGG_PATHWAYS_IN_CANCER, KEGG_FOCAL_ADHESION. Several significant pathways which were active in the low-risk group, including KEGG_PROPANOATE_METABOLISM, KEGG_CITRATE_CYCLE_TCA_CYCLE, KEGG_BETA_ALANINE_METABOLISM, KEGG_LONG_TERM_POTENTIATION, KEGG_LINOLEIC_ACID_METABOLISM (*Figure 13A*). The

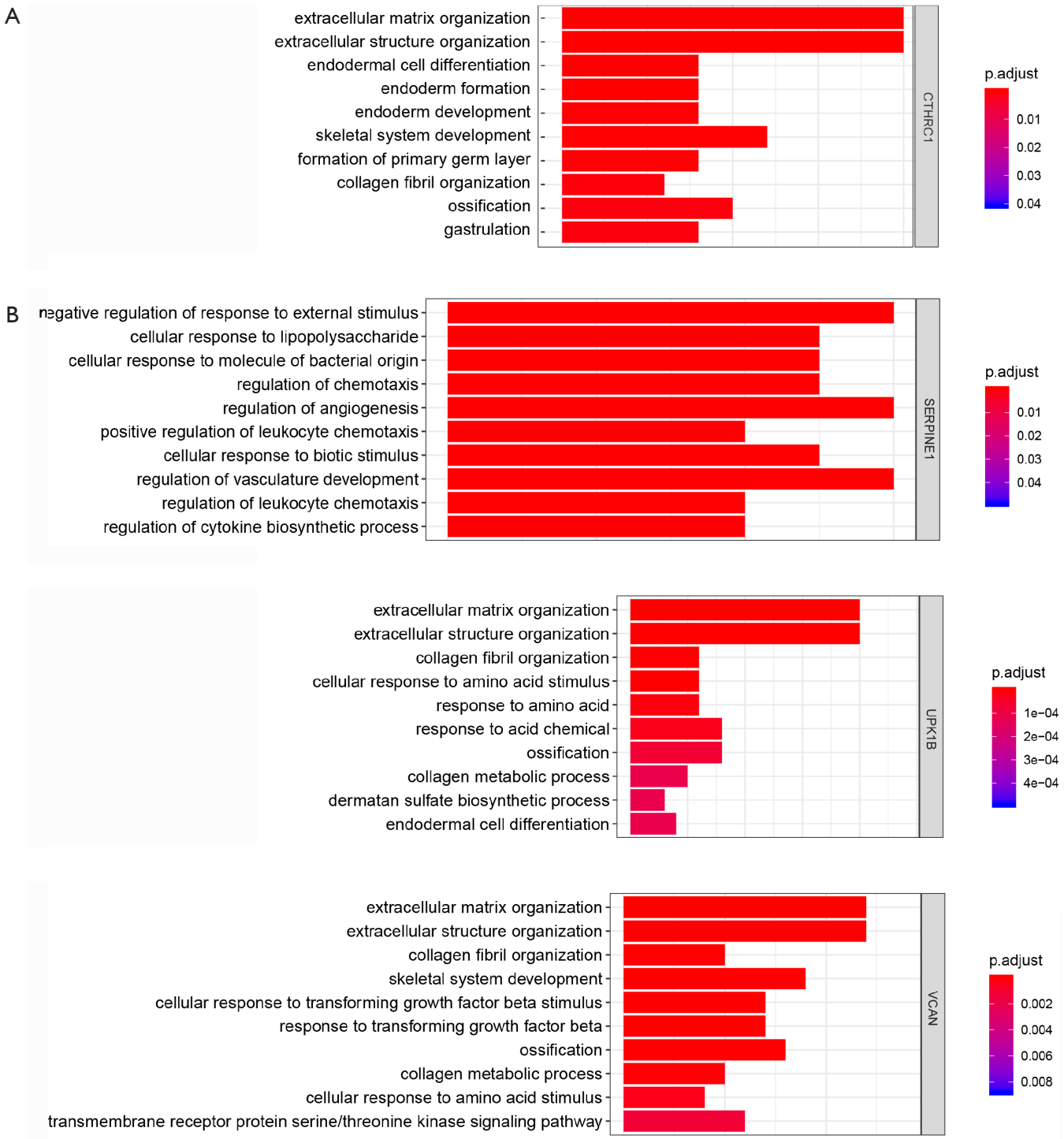

Figure 11 Potential biological processes for the key genes in GC. GC, gastric cancer.

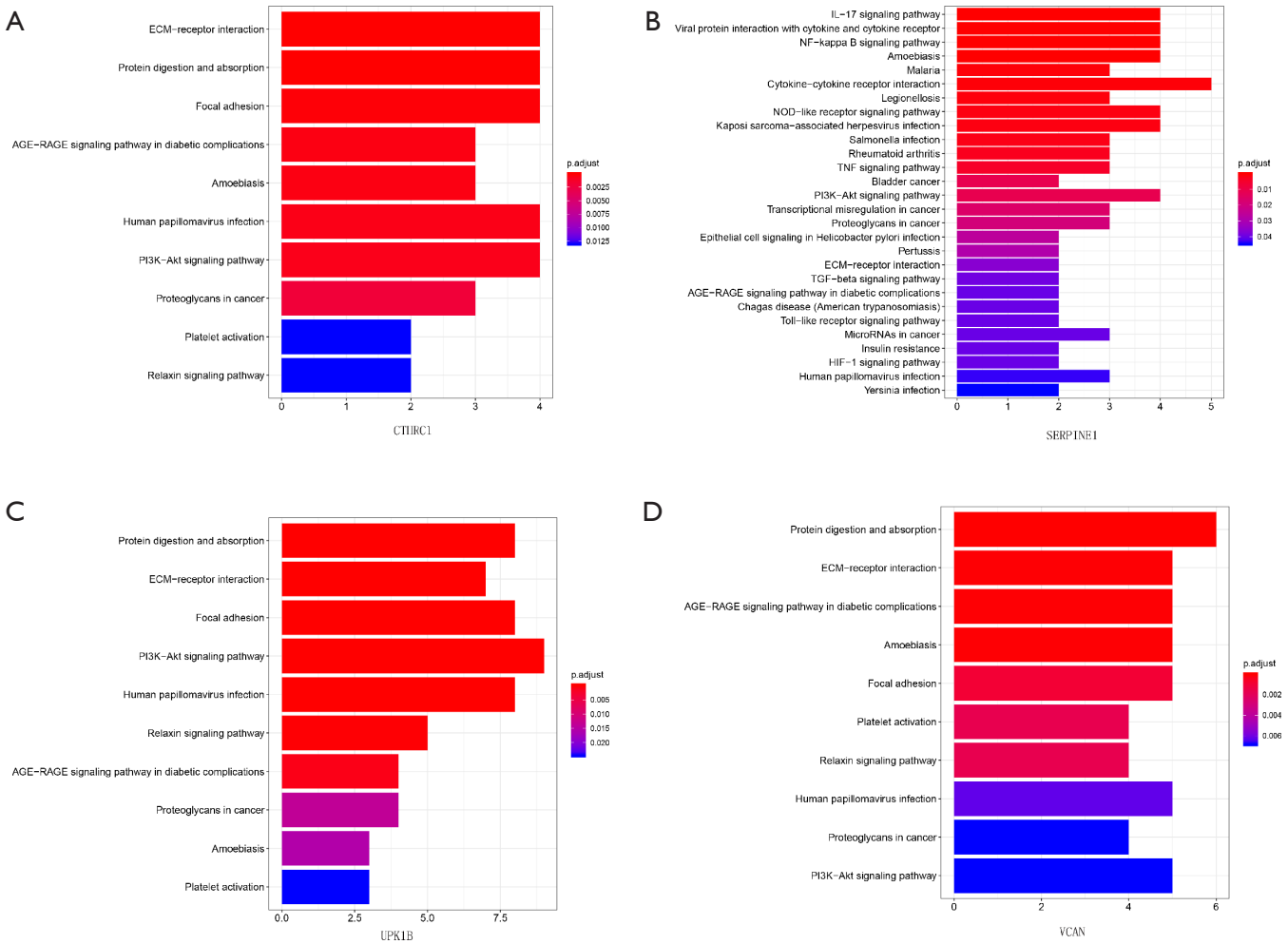

Figure 12 Potential signaling pathways for the key genes in GC. GC, gastric cancer.

most significant pathways were presented for *SERPINE1* (*Figure 13B*), *UPK1B* (*Figure 13C*) and *VCAN* (*Figure 13D*).

Discussion

GC is one most common malignant cancer worldwide and it is very difficult to treat the advanced-stage SC. Although the formation, progression and underlying mechanisms for GC have been revealed from some basic and clinical studies, the incidence and mortality of GC is still very high worldwide (10). Therefore, it is necessary to identify novel prognostic and therapeutic target for GC.

UPK1B is a structural protein on the surface of urothelial cells1, which was considered as the entirely specific for urothelium, recent studies have indicated that *UPK1B* also expressed in other tissues, including bladder, brain, eye, kidney, lung, stomach (11). *UPK1B* may promote the occurrence and development of cancer (12,13), *UPK1B* could promote the proliferation, invasion and metastasis in bladder cancer (14,15). Su *et al.* (16) showed abnormal expression of UPK1B in various types of cancers. However, the role of *UPK1B* in GC has not been reported. In this study, the different expression level between normal and cancer is of significance, high gene expression was significantly associated with a shorter OS, *UPK1B* is significant diagnostic factor in GC. The expression level was associated with distant metastasis, *UPK1B* may participate in the biological processes (extracellular matrix organization, collagen fibril organization, collagen metabolic process, endodermal cell differentiation) through ECM-receptor interaction, PI3K-Akt signaling pathway, relaxin signaling pathway to promote the metastasis in GC.

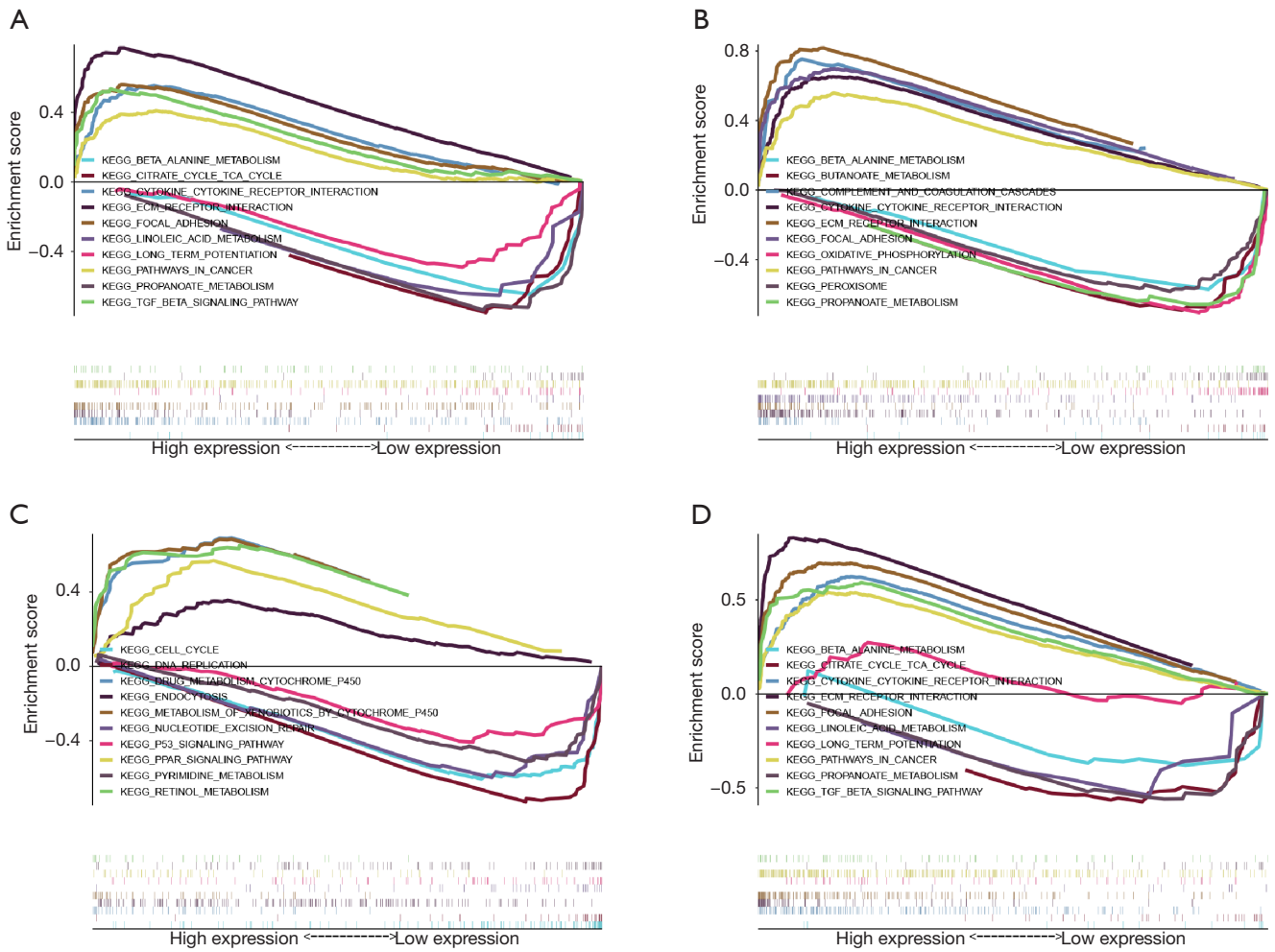

Figure 13 Enrichment plots from GSEA for (A) *CTHRC1*, (B) *SERPINE1*, (C) *UPK1B*, (D) *VCAN*. GSEA, gene set enrichment analysis; *CTHRC1*, collagen triple helix repeat containing 1; *SERPINE1*, plasminogen activator inhibitor type 1; *UPK1B*, uroplakin Ib; *VCAN*, Verscan.

The *CTHRC1* gene belongs to chromosome 8q22.3, which encoded a protein to participate in the vascularity and bone formation and so on (17). The expression level was different between normal tissue and tumor tissue for some types of tumors, including breast cancer (18), cervical cancer (19), colorectal cancer (20), liver cancer (21) and GC (22), the aberrant expression level was associated with poor OS and progression-free survival and it was the independent prognostic marker in GC in GC, which was consistent with our result. Recently, Ding *et al.* (23) have reported that HIF-1α/CXCR4 signaling may be involved in the migration and invasion in GC, however, the underlying molecular mechanism for *CTHRC1* promoting the occurrence and development of GC is not very clear. In this study, we identify several signaling pathway which may be involved in the occurrence and development of GC.

SERPINE1 gene encodes plasminogen activator inhibitor type 1, which participated in inhibiting tissue plasminogen activator and uridylyl phosphate adenosine, the aberrant expression in many types of cancer and *SERPINE1* could be an independent risk factor for various types of cancers, including head and neck cancer (24,25), esophageal cancer (26), bladder cancer (27), melanoma (28). Li *et al.* (29) indicated SERPINE1 is a poor prognosis for GC, and *SERPINE1* could promote tumour cell proliferation, migration, and invasion by regulating EMT. However, SERPINE1 still remains largely unknown in GC. In our study, *SERPINE1* was an significant diagnostic factor in GC, and we found

the expression level of *SERPINE1* was associated with depth of invasion, the potential signal pathways may participated in the biological process including NF-kappa B signaling pathway, PI3K-Akt signaling pathway, Toll-like receptor signaling pathway.

VCAN is a chondroitin sulfate proteoglycan, a member of the aggregating chondroitin sulfate PGs family, which is an important component of ECM (30). Verscan expression often occurs in the context of tissue remodeling, angiogenesis, including: follicular growth (31), inflammation (32), wound healing (33) or atherosclerotic lesions (34), and environmental significance around progressive tumors (35). It has been previously reported that tumor stromal cells play an important role in tumor formation and tumor progression (36), and *VCAN* is expressed and secreted by tumor stromal cells. Yeung *et al.* indicated that CAF-specific *VCAN* was up-regulated by TGF-β signal to promote tumorigenesis and invasion in ovarian cancer (37). The level of *VCAN* increased in many patients with malignant tumors includes colon cancer (38), rectal cancer (39), melanoma (40), odontogenic cancer (41), and ovarian cancer (42). In vitro and *in vivo* research, it has shown that *VCAN* can promote the proliferation, metastasis and invasion of cancer cells (43-45), with playing an important role in the formation of extracellular matrices that support tumor growth and metastasis. Shen *et al.* (46) reported that *VCAN* expression can be used as a prognostic indicator for GC patients, *VCAN* expression is higher in cancer tissues than in adjacent tissues, and could promote proliferation and invasion in GC cells. However, few literatures mentioned *VCAN* associated signaling pathways that promote the development of GC. We identified some signaling pathways that may be involved in the development of GC. This regulatory mechanism needs to be further elucidated.

Conclusions

In conclusion, by integrating four GEO and TCGA gene expression profile datasets, we identified four key genes (*CTHRC1*, *SERPINE1*, *VCAN*, *UPK1B)* which might as the novel potential prognostic molecular markers for GC. The four key genes have high prognostic performance, and could considered as independent prognostic factors for OS and DFS in GC. The four key genes act as oncogene to promote the development of GC, *CTHRC1* participated in endodermal cell differentiation, extracellular matrix organization, *SERPINE1* participated in regulation of angiogenesis, positive regulation of leukocyte chemotaxis cellular, regulation of vasculature development, *UPK1B* participated in extracellular matrix organization, collagen fibril organization, collagen metabolic process, endodermal cell differentiation, *VCAN* participated in extracellular matrix organization, cellular response to transforming growth factor beta stimulus. The study would provide some novel genes for the future prognosis prediction and potential molecular targeting therapy for GC.

However, further biological experiments should be performed to validate our results.

Acknowledgments

We are grateful to the reviewers for their constructive comments which led to improvements in this manuscript. In addition, thanks to Bin Zhao (Official Wechat Account: Bio_Med2017) of Xiamen University for suggestions on the manuscripts.

Funding: This study was supported by Xiamen Scientific and Technological Plan (No. 3502Z20194005).

Footnote

Conflicts of Interest: All authors have completed the ICMJE uniform disclosure form (available at http://dx.doi.org/10.21037/tcr-20-211). The authors have no conflicts of interest to declare.

Ethical Statement: The authors are accountable for all aspects of the work in ensuring that questions related to the accuracy or integrity of any part of the work are appropriately investigated and resolved.

References

1. Bertuccio P, Chatenoud L, Levi F, et al. Recent patterns in gastric cancer: a global overview. Int J Cancer 2009;125:666-73.

2. Ferro A, Peleteiro B, Malvezzi M, et al. Worldwide trends in gastric cancer mortality (1980-2011), with predictions to 2015, and incidence by subtype. Eur J Cancer 2014;50:1330-44.
3. Peleteiro B, Severo M, La Vecchia C, et al. Model-based patterns in stomach cancer mortality worldwide. Eur J Cancer Prev 2014;23:524-31.
4. Chen W. Cancer statistics: updated cancer burden in China. Chin J Cancer Res 2015;27:1.
5. Figueiredo C, Camargo MC, Leite M, et al. Pathogenesis of Gastric Cancer: Genetics and Molecular Classification. Curr Top Microbiol Immunol 2017;400:277-304.
6. He J, Jin Y, Chen Y, et al. Downregulation of ALDOB is associated with poor prognosis of patients with gastric cancer. Onco Targets Ther 2016;9:6099-109.
7. Oh SC, Sohn BH, Cheong JH, et al. Clinical and genomic landscape of gastric cancer with a mesenchymal phenotype. Nat Commun 2018;9:1777.
8. Hippo Y, Taniguchi H, Tsutsumi S, et al. Global gene expression analysis of gastric cancer by oligonucleotide microarrays. Cancer Res 2002;62:233-40.
9. Zhang X, Ni Z, Duan Z, et al. Overexpression of E2F mRNAs associated with gastric cancer progression identified by the transcription factor and miRNA co-regulatory network analysis. PLoS One 2015;10:e0116979.
10. Siegel RL, Miller KD, Jemal A. Cancer statistics, 2019. CA Cancer J Clin 2019;69:7-34.
11. Yu J, Lin JH, Wu XR, et al. Uroplakins Ia and Ib, two major differentiation products of bladder epithelium, belong to a family of four transmembrane domain (4TM) proteins. J Cell Biol 1994;125:171-82.
12. Webb GC, Finch JL, Cowled PA. Assignment of the Uroplakin 1b (Upk1b) gene to mouse chromosome 16 bands B5-C2 by in situ hybridization. Cytogenet Cell Genet 1999;84:37-8.
13. Finch JL, Webb GC, Evdokiou A, et al. Chromosomal localization of the human urothelial "tetraspan" gene, UPK1B, to 3q13.3-q21 and detection of a TaqI polymorphism. Genomics 1997;40:501-3.
14. Osman I, Kang M, Lee A, et al. Detection of circulating cancer cells expressing uroplakins and epidermal growth factor receptor in bladder cancer patients. Int J Cancer 2004;111:934-9.
15. Olsburgh J, Harnden P, Weeks R, et al. Uroplakin gene expression in normal human tissues and locally advanced bladder cancer. J Pathol 2003;199:41-9.
16. Su J, Zhang Y, Su H, et al. A recurrence model for laryngeal cancer based on SVM and gene function clustering. Acta Otolaryngol 2017;137:557-62.
17. Takeshita S, Fumoto T, Matsuoka K, et al. Osteoclast-secreted CTHRC1 in the coupling of bone resorption to formation. J Clin Invest 2013;123:3914-24.
18. Lai YH, Chen J, Wang XP, et al. Collagen triple helix repeat containing-1 negatively regulated by microRNA-30c promotes cell proliferation and metastasis and indicates poor prognosis in breast cancer. J Exp Clin Cancer Res 2017;36:92.
19. Li N, Chen L, Liu C, et al. Elevated CTHRC1 expression is an indicator for poor prognosis and lymph node metastasis in cervical squamous cell carcinoma. Hum Pathol 2019;85:235-41.
20. Ni S, Ren F, Xu M, et al. CTHRC1 overexpression predicts poor survival and enhances epithelial-mesenchymal transition in colorectal cancer. Cancer Med 2018;7:5643-54.
21. Zhou H, Su L, Liu C, et al. CTHRC1 May Serve As A Prognostic Biomarker For Hepatocellular Carcinoma. Onco Targets Ther 2019;12:7823-31.
22. Gu L, Liu L, Zhong L, et al. Cthrc1 overexpression is an independent prognostic marker in gastric cancer. Hum Pathol 2014;45:1031-8.
23. Ding X, Huang R, Zhong Y, et al. CTHRC1 promotes gastric cancer metastasis via HIF-1alpha/CXCR4 signaling pathway. Biomed Pharmacother 2020;123:109742.
24. Pavon MA, Arroyo-Solera I, Cespedes MV, et al. uPA/uPAR and SERPINE1 in head and neck cancer: role in tumor resistance, metastasis, prognosis and therapy. Oncotarget 2016;7:57351-66.
25. Pavon MA, Arroyo-Solera I, Tellez-Gabriel M, et al. Enhanced cell migration and apoptosis resistance may underlie the association between high SERPINE1 expression and poor outcome in head and neck carcinoma patients. Oncotarget 2015;6:29016-33.
26. Klimczak-Bitner AA, Kordek R, Bitner J, et al. Expression of MMP9, SERPINE1 and miR-134 as prognostic factors in esophageal cancer. Oncol Lett 2016;12:4133-8.
27. Zhang G, Gomes-Giacoia E, Dai Y, et al. Validation and clinicopathologic associations of a urine-based bladder cancer biomarker signature. Diagn Pathol 2014;9:200.
28. Klein RM, Bernstein D, Higgins SP, et al. SERPINE1 expression discriminates site-specific metastasis in human melanoma. Exp Dermatol 2012;21:551-4.
29. Li L, Zhu Z, Zhao Y, et al. FN1, SPARC, and SERPINE1 are highly expressed and significantly related to a poor prognosis of gastric adenocarcinoma revealed by microarray and bioinformatics. Sci Rep 2019;9:7827.

30. Schwartz NB, Pirok EW, 3rd, Mensch JR, Jr., et al. Domain organization, genomic structure, evolution, and regulation of expression of the aggrecan gene family. Prog Nucleic Acid Res Mol Biol 1999;62:177-225.
31. Russell DL, Ochsner SA, Hsieh M, et al. Hormone-regulated expression and localization of versican in the rodent ovary. Endocrinology 2003;144:1020-31.
32. Hakkinen L, Westermarck J, Kahari VM, et al. Human granulation-tissue fibroblasts show enhanced proteoglycan gene expression and altered response to TGF-beta 1. J Dent Res 1996;75:1767-78.
33. Cattaruzza S, Schiappacassi M, Ljungberg-Rose A, et al. Distribution of PG-M/versican variants in human tissues and de novo expression of isoform V3 upon endothelial cell activation, migration, and neoangiogenesis in vitro. J Biol Chem 2002;277:47626-35.
34. Evanko SP, Raines EW, Ross R, et al. Proteoglycan distribution in lesions of atherosclerosis depends on lesion severity, structural characteristics, and the proximity of platelet-derived growth factor and transforming growth factor-beta. Am J Pathol 1998;152:533-46.
35. Crowther M, Brown NJ, Bishop ET, et al. Microenvironmental influence on macrophage regulation of angiogenesis in wounds and malignant tumors. J Leukoc Biol 2001;70:478-90.
36. Calon A, Lonardo E, Berenguer-Llergo A, et al. Stromal gene expression defines poor-prognosis subtypes in colorectal cancer. Nat Genet 2015;47:320-9.
37. Yeung TL, Leung CS, Wong KK, et al. TGF-beta modulates ovarian cancer invasion by upregulating CAF-derived versican in the tumor microenvironment. Cancer Res 2013;73:5016-28.
38. Theocharis AD. Human colon adenocarcinoma is associated with specific post-translational modifications of versican and decorin. Biochim Biophys Acta 2002;1588:165-72.
39. Tsara ME, Theocharis AD, Theocharis DA. Compositional and structural alterations of proteoglycans in human rectum carcinoma with special reference to versican and decorin. Anticancer Res 2002;22:2893-8.
40. Touab M, Villena J, Barranco C, et al. Versican is differentially expressed in human melanoma and may play a role in tumor development. Am J Pathol 2002;160:549-57.
41. Ito Y, Abiko Y, Tanaka Y, et al. Immunohistochemical localization of large chondroitin sulfate proteoglycan in odontogenic tumor. Med Electron Microsc 2002;35:173-7.
42. Voutilainen K, Anttila M, Sillanpaa S, et al. Versican in epithelial ovarian cancer: relation to hyaluronan, clinicopathologic factors and prognosis. Int J Cancer 2003;107:359-64.
43. Ang LC, Zhang Y, Cao L, et al. Versican enhances locomotion of astrocytoma cells and reduces cell adhesion through its G1 domain. J Neuropathol Exp Neurol 1999;58:597-605.
44. Zhang Y, Cao L, Yang BL, et al. The G3 domain of versican enhances cell proliferation via epidermial growth factor-like motifs. J Biol Chem 1998;273:21342-51.
45. Yang BL, Zhang Y, Cao L, et al. Cell adhesion and proliferation mediated through the G1 domain of versican. J Cell Biochem 1999;72:210-20.
46. Shen XH, Lin WR, Xu MD, et al. Prognostic significance of Versican expression in gastric adenocarcinoma. Oncogenesis 2015;4:e178.

Cite this article as: Zhu Z, Xu J, Li L, Ye W, Chen B, Zeng J, Huang Z. Comprehensive analysis reveals *CTHRC1*, *SERPINE1*, *VCAN* and *UPK1B* as the novel prognostic markers in gastric cancer. Transl Cancer Res 2020;9(7):4093-4110. doi: 10.21037/tcr-20-211

Table S1 Twenty-three survival related genes were identified by performing the Kaplan-Meier analysis (P<0.05)

Gene	P value
SERPINE1	0.000219
UPK1B	0.001473
ANGPT2	0.005681
AADAC	0.006003
PDGFRB	0.01205
TNFRSF11B	0.012199
OLFML2B	0.012447
LOX	0.013269
SMPD3	0.013456
VCAN	0.01891
MAMDC2	0.020227
ECT2	0.020561
TUBB6	0.02132
MFAP2	0.022236
DPT	0.025029
COL4A1	0.027449
COL5A2	0.028342
CTHRC1	0.029945
FAP	0.040863
AGT	0.04225
MAP7D2	0.047641
MMP12	0.048191
COL12A1	0.049813
OSMR	0.054358
CALD1	0.059583
INHBA	0.067962
CST2	0.071974
CLIC6	0.082916
COL10A1	0.084384
S100A9	0.096072
GUCA2B	0.096917
COL1A1	0.109207
COL5A1	0.10969
COL6A1	0.11083
COL3A1	0.111259
SYTL5	0.114856
CDH11	0.124127
ADH7	0.130015
VSIG1	0.132332
SCIN	0.13247
SPP1	0.13646
PLLP	0.13804
PRC1	0.147127
C6orf58	0.147472
CIDEC	0.151807
ESM1	0.15414
BCAT1	0.155191
LTF	0.157024
MT1G	0.158712
PI15	0.158844
OTC	0.164052
UGT2B15	0.174819
TREM1	0.184753
SOSTDC1	0.187739
EMP3	0.189071
PDIA2	0.189871
COL14A2	0.191785
OLR1	0.205573
RNASE1	0.20733
ASPN	0.212696
TFF2	0.233068
SULF1	0.238557
MT1M	0.247873
ETV4	0.254438
KRT20	0.265582
FBP2	0.265783
GHRL	0.270264
ANXA10	0.276172
MAOA	0.276519
AKR7A3	0.276782
PBK	0.277451
SNX10	0.28286
TNFSF4	0.290801
KCNJ15	0.29299
GKN1	0.29894
SELENBP1	0.306575
CHI3L1	0.311321
RDH12	0.320753
CXCL17	0.324846
HRASLS2	0.327991
OLFM4	0.32988
FSCN1	0.358197
CPXM1	0.364493
FBXO32	0.36483
SFRP4	0.369919
MMP1	0.372373
GEM	0.383342
LIFR	0.391984
IRX3	0.395766
GKN2	0.399234
THY1	0.40806
CA2	0.41812
GGT6	0.431151
AQP9	0.43801
CXCL5	0.443691
VILL	0.446059
HOXC6	0.450283
ECM1	0.453289
APOBEC2	0.455273
THBS2	0.469881
CLDN2	0.473161
RCN3	0.481199
WNT2	0.489813
CBR1	0.49536
CHGA	0.503973
APOE	0.506067
CCL18	0.506183
IGF2BP3	0.510406
GSTA1	0.511807
TIMP1	0.51665
RARRES1	0.525777
KLK6	0.532234
SPINK7	0.533784
MAL	0.541585
S100A8	0.548391
SST	0.550388
CEACAM6	0.552092
COL11A1	0.556812
TAGLN	0.562203
LYSE	0.563069
MT1H	0.568436
KLK11	0.569524
SSTR1	0.573811
PMEPA1	0.583951
MXRA5	0.584339
CXCL9	0.587203
TFF1	0.596394
EPHB2	0.597971
PLK1	0.600849
CDH3	0.605368
MSR1	0.612339
F2RL2	0.616396
C1orf116	0.617585
S100P	0.617652
BGN	0.624311
SERPINH1	0.629089
FPR3	0.634469
CYP4F12	0.653012
CAP2	0.654383
MMP3	0.655905
TOP2A	0.657755
ANLN	0.658936
REG3A	0.660342
KCNE2	0.66711
PGC	0.668703
SCNN1B	0.6804
ALDH3A1	0.685418
CCKBR	0.685544
MLLT11	0.687678
CYP2C9	0.69351
SULT2A1	0.694968
ADH1C	0.70767
PSCA	0.709882
PLA2G2A	0.712788
IFITM1	0.71556
LIPF	0.717355
LIF	0.724972
CLDN1	0.734878
LDHD	0.740984
PIGR	0.743844
KLF4	0.744254
SLC16A9	0.745095
PLAU	0.745453
CAPN9	0.747822
PBLD	0.753745
TRIP13	0.754745
CXCL1	0.768736
GIF	0.780016
TCN1	0.781361
C4BPA	0.78778
TPX2	0.791127
APOBEC1	0.802589
GATA5	0.812229
SLC28A2	0.819387
SIDT2	0.827656
ANG	0.828256
CST1	0.83539
SCGB2A1	0.849791
ATP4A	0.857416
MMP7	0.857637
CXCL10	0.865142
FMO5	0.885593
TNFRSF17	0.887868
SULT1B1	0.89062
PLA2G7	0.892582
FAM3B	0.897619
CAPN13	0.910593
LIPG	0.911736
GAST	0.919055
CKB	0.925075
ALDOB	0.928519
AKR1C3	0.935679
MMP9	0.938571
ITPKA	0.948574
FCGBP	0.952871
VSIG2	0.954352
BCAS1	0.957483
HPGD	0.960429
PXMP2	0.966763
CYP2C18	0.969566
ATP4B	0.970968
CILP	0.971054
TMED6	0.996557